Thermally Enhanced Cable Insulation for the Nb-Ti High Luminosity LHC Inner Triplet Model

Pier Paolo Granieri, Paolo Fessia, David Richter, and Davide Tommasini

***Abstract*—A new concept of polyimide electrical insulation for superconducting cables of accelerator magnets was developed in the last years. Its enhanced He II permeability allows a significant improvement of the heat extraction from the coil. This cable insulation concept is used for the quadrupole magnet prototype for the insertion region of the High Luminosity—Large Hadron Collider project. It aims at pushing the limits of the Nb-Ti technology to withstand high heat deposition.**

Cable samples wrapped with the new insulation scheme were characterized from the thermal standpoint, as well as from the electrical and mechanical ones. In particular, heat transfer measurements from insulated cables towards the helium cooling bath were performed in a coil-like configuration. Various wrapping schemes were tested in different mechanical conditions, and a model was developed to explain the experimental results. The paper summarizes the main results of all these investigations.

***Index Terms*—Accelerator superconducting magnets, cable insulation, He II heat transfer, LHC upgrade.**

I. Introduction

THE CABLE electrical insulation of superconducting accelerator magnets must combine robust dielectric properties with sufficient heat extraction to maintain them superconducting in case of heat deposit in the coil. In case of the Nb-Ti magnets of the Large Hadron Collider (LHC), the compromise was found by leaving a 2 mm gap between adjacent turns of the last insulation layer [1]. In this way channels for the He II coolant are created between insulated adjacent cables, thus providing larger heat evacuation with respect to sealed insulation schemes [2].

Superconducting magnets having to withstand larger heat loads than in the current LHC operation need more efficient heat extraction from the coil. This is the case of the inner triplets of the High Luminosity LHC (HL-LHC) upgrade project, which will replace the existing quadrupole magnets in the ATLAS and CMS insertion regions [3]. One single upgrade will be realized, instead of the initially scheduled two phases, that will rely either on the Nb_3Sn or on the Nb-Ti technology. If used at the same current density and magnetic field as the Nb-Ti, the Nb_3Sn option can provide a larger temperature margin. This advantage is considerably reduced if the heat extraction capability of the Nb-Ti coils is improved by acting on the cable electrical insulation [4]. This represents indeed the thermal bottleneck of the coil, and in particular of the inner layer which is the most exposed to beam loss [5].

Manuscript received September 13, 2011; accepted December 12, 2011. Date of publication January 11, 2012; date of current version May 24, 2012.

P. P. Granieri is with the Technology Department, CERN, Geneva 1211, Switzerland, and is also with the Particle Accelerator Physics Laboratory (LPAP), Swiss Federal Institute of Technology (EPFL), Lausanne 1015, Switzerland (e-mail: Pier.Paolo.Granieri@cern.ch).

P. Fessia, D. Richter, and D. Tommasini are with the Technology Department, CERN, Geneva 1211, Switzerland.

Color versions of one or more of the figures in this paper are available online at http://ieeexplore.ieee.org.

Digital Object Identifier 10.1109/TASC.2012.2183669

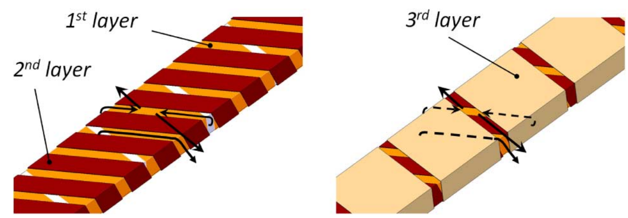

Fig. 1. Sketch of the EI wrapping pattern: first two layers (left) and all three layers (right). The directions of the He II heat fluxes are also shown.

An innovative cable insulation scheme, hereafter referred to as Enhanced Insulation (EI), was developed to significantly improve the heat transfer between Nb-Ti cables and He II bath [6]. It is being used for wrapping the cables of the 120 mm wide aperture quadrupole magnet prototype for the HL-LHC [3].

This paper summarizes the EI features and the systematic investigations performed on cables stack samples to characterize it. The comparison to the LHC standard insulations is shown, in particular with respect to the insulation of the Main Bending (MB) dipole magnets. The results of heat transfer measurements and relevant modeling of different variants of EI are presented. The underlying thermal mechanisms are highlighted, as well as the dependence on the applied pressure that tends to close the channels. The main results of the electrical and mechanical tests are reported.

II. Enhanced Insulation Pattern

The EI is made of three polyimide layers, the first and the last of which wrapped in the same direction whereas the second one is cross-wrapped in the opposite direction. The scheme has evolved from the initial versions [4] and [7], to enable the automatic wrapping of commercially available tapes. The standard EI scheme [6], shown in Fig. 1, is defined as follows:

1) The 1st layer is 9 mm wide and 50 μm thick. It is wound with 1 mm spacing;
2) The 2nd layer is 3 mm wide and 75 μm thick. It is wound with 1.5 mm spacing;
3) The 3rd tape is 9 mm wide and 69 μm thick. It is wound with 1 mm spacing, featuring a 50% "spaced overlap" with the 1st layer.

Alternatives to this layout that are mentioned in the paper feature variation of one single parameter with respect to the above mentioned ones. In the following, only the modified parameter will be mentioned.

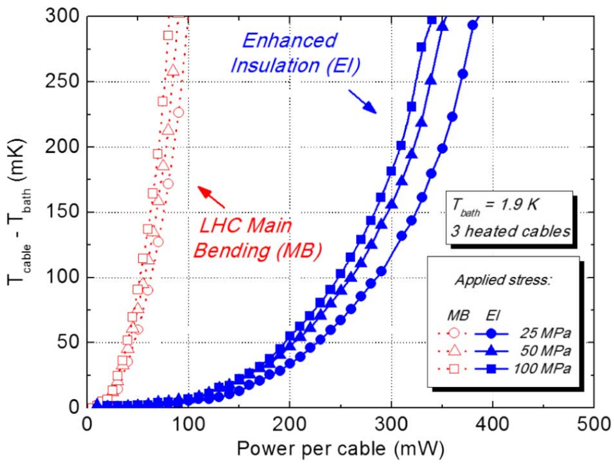

Fig. 2. Temperature rise of central cable vs. heat load for EI and MB insulation schemes at different pressure levels in 1.9 K He II bath (from [6]).

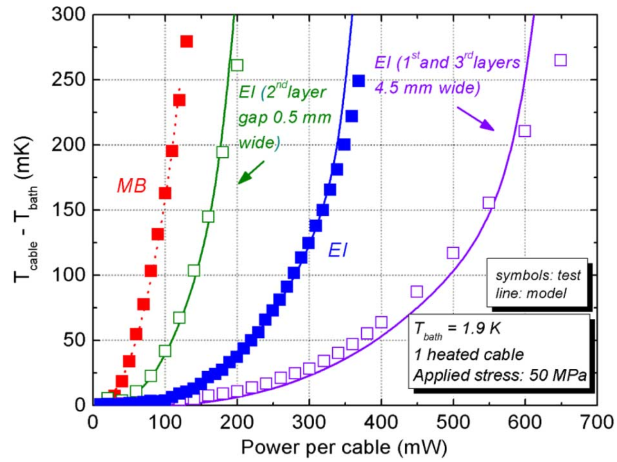

Fig. 3. Temperature rise of central cable vs. heat load for three variants of EI and MB insulation schemes in 1.9 K He II bath, model (curves) vs. measurements (markers).

The main innovations of the EI pattern consist in the channels created along the 2nd layer and in the openings between layers 1 and 2 as well as between layers 2 and 3, which allow a direct path from the strands to the bath. Since the cables are piled up on their large side, the channels can have different lengths. They can either come out in the cable small side, hence directly to the bath, or in the cable large side. In the latter case, a supplementary channel length has to be considered, along the edges of the 3rd layer, before reaching the bath. The described He II heat paths are shown in Fig. 1.

The samples we refer to throughout the paper are prepared by alternately stacking a number of insulated cables, ranging from 2 to 10, in order to compensate for the keystone angle and to form a rectangular stack. As in the coil, the polyimide glue on the outer surface of the 3rd insulation layer reacts during the curing cycle thus providing cohesion between adjacent cables. Two different curing cycles are realized, at a pressure of 80 or 130 MPa and at a temperature of 190°C.

III. Heat Transfer

A. He II Cooling

The heat transfer test procedure is detailed in [6]. The samples are made of $\mathrm{CuNi_{10\ wt\%}}$ resistive cables with the same geometry as the LHC Cable 01 [1], which are heated up by Joule effect. They are cured at 130 MPa and instrumented with $\mathrm{AuFe_{0.07\ at\%}}$-Chromel thermocouple junctions. The results reported in the paper refer to the sensors located in the middle of one of the two central cables.

Fig. 2 reports the results of the EI vs. MB insulation, in terms of steady-state temperature difference between middle cable and bath as a function of the power dissipated in the 156 mm long cable. The three central cables of the stack are heated up simultaneously. In the experimental setup, both cables small sides are directly cooled by pressurized He II bath at 1.9 K. Different compressive pressures of 50, 75 and 100 MPa are applied at room temperature and held during the test. Because of the differential thermal contractions, it was measured that they correspond to higher pressures at low temperature [6], e.g. 100 MPa at 300 K corresponds to about the pressure of 118 MPa on the coil mid-plane during powering [3].

The heat extraction through the enhanced insulation at a fixed temperature proved to be at least four times more efficient than through the LHC standard insulation. This feature holds at the highest applied pressure, despite the reduction of the channels size. In fact the heat extraction tends to an asymptote for high pressures. It was also observed that adjacent cables insulated with the EI are thermally decoupled to each other [6].

The EI can provide such an improved heat transfer thanks to the large amount of He II made available by the channels directly linking strands to bath. A fully developed turbulent regime is established in the channels, as shown in [8].

Since the projection of the channels in the cable transversal direction is longer than the height of the cable small side, every channel lies on the cable large side for most of its length. In this zone it is submitted to the pressure applied on the cable large sides, hence all the channels feature the same minimum cross-section. For this reason the heat transfer contribution of the large side will not be differentiated from that of the small side. This is not the case of the LHC standard insulation, where the mechanical pressure only has an impact on the channels (slits) located on the large side [9].

Simple models based on these considerations allow simulating the tests, describing coupled helium and polyimide solid conduction heat transfer. Fig. 3 reports the comparison between test and model for MB, standard EI and two variants of EI each featuring one different geometrical parameter with respect to the standard EI. In one variant the 2nd layer is wound with 0.5 mm spacing (instead of 1.5 mm), whereas in the other variant the 1st and 3rd layers are 4.5 mm wide (instead of 9 mm). The latter features an even more efficient heat extraction than the standard EI. However these variants are not intended to substitute the standard EI, but to provide indications on the most significant parameters for the heat extraction and to validate the model. The details of the thermal models will be presented in a dedicated publication [9].

The main geometrical parameters affecting the EI heat transfer are the channels length and cross-section, as well as the number of openings between the 2nd and the 1st/3rd insulation layer. The minimum length of the channels, i.e. in case they end on the cable small side, ranges from 6 to 10 mm depending on the EI variant. The increased length of the channels ending

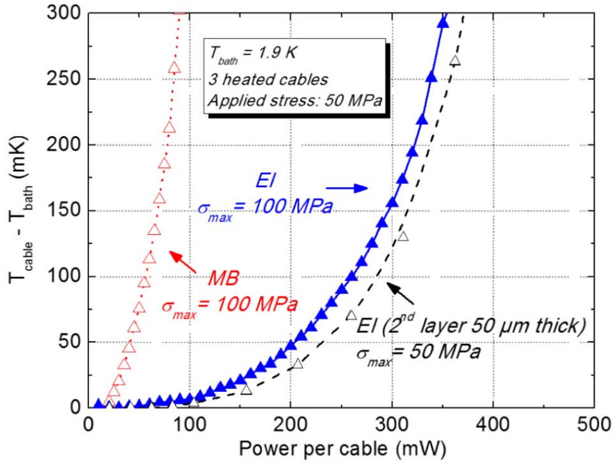

Fig. 4. Temperature rise of central cable vs. heat load for two variants of EI and MB insulation schemes in 1.9 K He II bath, for different maximum pressure seen by the samples.

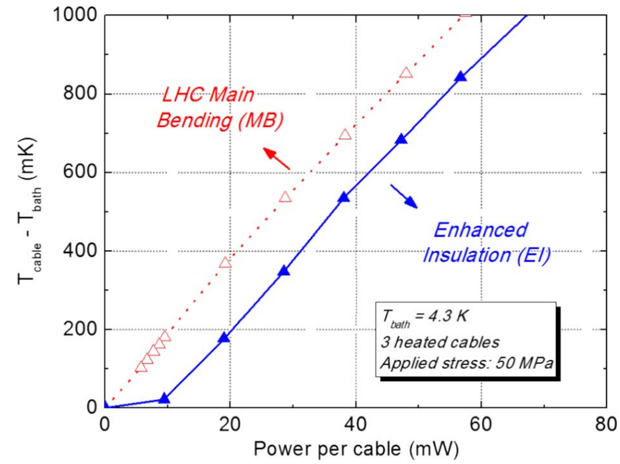

Fig. 5. Temperature rise of central cable vs. heat load for EI and MB insulation schemes in 4.3 K He I bath.

on the cable large side is taken into account. The number of openings ranges between 50 and 60 in the measured samples. The channels cross-section is an unknown parameter featuring a non linear dependence on the applied pressure, on the maximum pressure seen by the sample, on the curing cycle and on creep mechanisms. It is therefore hard to define. Once the other parameters are set according to the specific layout, we use the channels cross-section as fitting parameter. In Fig. 3, in case of an applied pressure of 50 MPa, a good agreement between tests and model is found with values ranging between 40% and 60% of the geometrical (without applied pressure) channels cross-section.

B. Micro-Channels

In order to provide a fundamental understanding of the insulation underlying thermal mechanisms, an experimental setup was built to investigate heat transport through pressurized He II micro-channels, where deviations from theory can appear. Micro electro-mechanical technologies are employed to realize channels with thickness of dozens of μm. The first results are reported in [10]. They confirm the independence of the turbulent heat transfer on the shape and size down to a dimension of 100 μm. For smaller dimensions, the laminar regime could be identified, as well as the critical heat flux corresponding to its end that shows a peak at a bath temperature of around 1.9 K. Further investigations are ongoing to address smaller channels. These results will constitute a basis for the modeling of the heat transfer through superconducting cable insulation.

C. Effect of Mechanical Pressure

As shown in [6] and mentioned in Section III-A, the pressure applied during the test has a significant impact on the heat transfer through the insulation. The dependence of the cable behavior on its position in the coil defining the applied pressure after powering should therefore be considered.

There are also other mechanical effects influencing the channels size. For the samples analyzed so far, the maximum pressure applied after the curing cycle was always 100 MPa. Fig. 4 shows the comparison of the already presented MB and standard EI curves to another variant of EI that was cycled up to only 50 MPa. Despite the smaller thickness of the 2nd insulation layer (50 instead of 75 μm), resulting in a smaller channels cross-section, the heat extraction is larger than in the standard EI. This result can be explained because of the smaller plastic deformation, which will be addressed from the mechanical point of view in Section V. The maximum pressure in all the other reported measurements is 100 MPa.

Plastic deformation is also induced by the creep mechanism. Since its effect is more evident during the first days [11], our testing procedure leaves enough time for it to act [6]. On the other hand the effect of the curing was not investigated but might be not negligible. The curing cycle used for our samples is conservative with respect to the expected curing pressure of 50 MPa [3]. Evaluating the impact of this parameter would require an experimental verification.

D. He I Cooling

Although not the primary aim of the EI, the heat extraction in 4.3 K He I cooling bath was measured. As shown in Fig. 5 even in this case the EI provides an improvement with respect to MB, though smaller and only significant for small heat deposit. This behavior is associated to the larger amount of He in contact with the strands, thus a larger heat transfer is needed to reach the critical heat flux for film boiling formation.

IV. Dielectric Strength

Electrical tests on cables stacks cured at 130 MPa were performed in air under a compressive pressure of 80 MPa [11]. Though smaller than that of MB, the measured breakdown voltage of the EI is larger than 11 kV. The results of previous tests carried out on different EI schemes [7] confirm these values. The robustness of the electrical protection provided by the overlapped 1st and 3rd layer is then validated on cables samples.

V. Mechanical Behavior

The mechanical characterization of the EI was performed in order to determine the final parameters for coil curing and shim size. It is reported in [11]. It is worth noting the good agreement found between these measurements performed on cables stacks with respect to arch measurements [3].

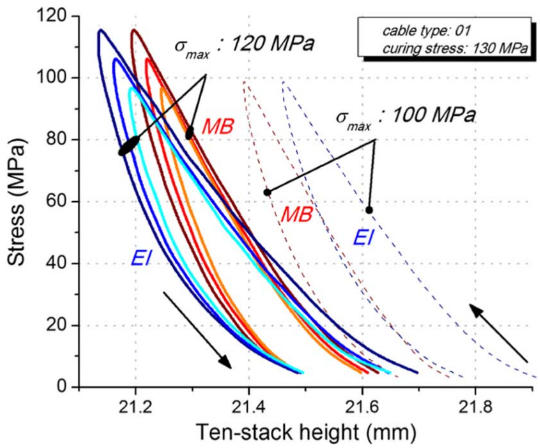

Fig. 6. Pressure vs. height of the EI and MB stacks, for different values of the maximum pressure seen by the samples.

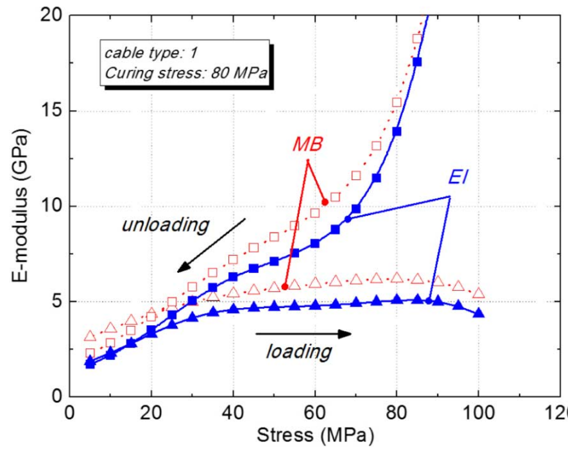

Fig. 7. Stack Elastic modulus vs. pressure for the loading and unloading branches of EI and MB insulation schemes.

The insulation thickness was measured for different insulation schemes, curing pressures and cable types. The insulation thickness loss after curing is larger for the EI with respect to MB because of the higher void fraction and of the higher peak stresses originated at the crossing of the different insulation layers.

The pressure losses due to polyimide creep were analyzed, showing that the largest losses take place during the first days after the beginning of the test. The behavior of the EI is similar to the MB insulation for the LHC cable 01 type, whereas it presents larger relaxation when applied on the more compacted LHC cable 02 type [1]. This behavior was explained considering two different mechanisms of stress relaxation, occurring either between cable and 1st insulation layer or between layers. The first one is dominant for the MB insulation, whereas the second one is dominant for the EI schemes. It was also shown that a higher curing pressure helps stabilizing the cable, pre-creeping the stack during curing.

The effect of the maximum pressure seen by the cable, which influence on the heat transfer was shown in Section III-C, is reported in Fig. 6. A plastic deformation occurs when exceeding the maximum pressure of 100 MPa, for MB and EI. On the other hand the loading branches of the different cycles nearly superpose if the maximum pressure is not exceeded.

Fig. 7 reports the measured elastic modulus as a function of the applied pressure for MB vs. EI, during loading and unloading. The curing pressure was in this case 80 MPa, whereas the LHC cable 01 type was the same as in the reported thermal and electrical tests. The EI features an approximately 10% softer behavior than the MB insulation.

VI. Conclusion

Thermally enhanced cable insulation schemes represent an interesting option for Nb-Ti cables to become more performing from the thermal standpoint than $\mathrm{Nb_3Sn}$ cables. They allow a considerable heat transfer thanks to the big channels permeating their internal structure and directly linking the strands to the He II bath.

The standard enhanced insulation scheme used for the HL-LHC prototype provides an about four times larger heat extraction with respect to the current LHC insulation. Recent tests performed on variants of this scheme showed that there is potential for further improving the insulation, provided that the electrical robustness is ensured. A heat transfer model was developed to explain the experimental tests, featuring good agreement with the measurements and allowing identifying the relevant mechanisms.

Further experimental tests showed the dependence of the insulation thermal properties on the applied pressure and on the peak pressure. Furthermore, systematic investigations on cables stacks allowed describing also the electrical and mechanical behavior of such insulation schemes.

Acknowledgment

The authors thank L. Bottura for his support, S. Luzieux for insulating and curing the samples, as well as B. Colijn and J. van Nugteren for the help in the computer simulations.

References

[1] LHC Design Report Vol. 1 CERN. Geneva, CH, 2004.
[2] C. Meuris, B. Baudouy, D. Leroy, and B. Szeless, "Heat transfer in electrical insulation of LHC cables cooled with superfluid helium," *Cryogenics*, vol. 39, pp. 921–931, September 1999.
[3] G. Kirby *et al.*, "Engineering design and manufacturing challenges for a wide-aperture, superconducting quadrupole magnet," *IEEE Trans. Appl. Supercond.*, submitted for publication.
[4] M. La China and D. Tommasini, "A comparative study of heat transfer from Nb-Ti and $\mathrm{Nb_3Sn}$ coils to He II," *Phys. Rev. Spec. Top. Accel. Beams*, vol. 11, August 2008.
[5] F. Cerutti, M. Mereghetti, and E. Wildner, Update of Power Deposition Studies in the LHC Upgrade Phase I Insertion Regions EDMS 975134, CERN. Geneva, Switzerland, 2008.
[6] P. P. Granieri, P. Fessia, D. Richter, and D. Tommasini, "Heat transfer in an enhanced cable insulation scheme for the superconducting magnets of the LHC luminosity upgrade," *IEEE Trans. Appl. Supercond.*, vol. 20, pp. 168–171, June 2010.
[7] D. Tommasini and D. Richter, "A new cable insulation scheme improving heat transfer in Nb-Ti superconducting accelerator magnets," in *Proc. 11th European Particle Accelerator Conference*, Genoa, 2008.
[8] P. P. Granieri and D. Richter, "Heat transfer measurements through thermally enhanced insulation schemes for Nb-Ti superconducting magnets operating in He II," in *Proc. of the 23rd ICEC and ICMC 2010*, Wroclaw, 2010, pp. 893–898.
[9] P. P. Granieri, "Heat transfer through cable insulation of Nb-Ti superconducting magnets operating in He II," *Cryogenics*, to be published.
[10] P. P. Granieri and B. Baudouy *et al.*, "Steady-state heat transfer through micro-channels in pressurized He II," *Advances in Cryogenic Engineering*, to be published.
[11] P. Fessia and P. P. Granieri *et al.*, "Electrical and mechanical performance of an enhanced cable insulation scheme for superconducting magnets," *IEEE Trans. Appl. Supercond.*, vol. 20, pp. 1622–1625, June 2010.